

# PLOS Neglected Tropical Diseases

## Paper-based ELISA diagnosis technology for human brucellosis based on a multiepitope fusion protein --Manuscript Draft--

<b>Manuscript Number:</b>	PNTD-D-21-00330
<b>Full Title:</b>	Paper-based ELISA diagnosis technology for human brucellosis based on a multiepitope fusion protein
<b>Short Title:</b>	P-ELISA for diagnosing human brucellosis
<b>Article Type:</b>	Research Article
<b>Keywords:</b>	brucellosis; nano-zinc oxide; p-ELISA; immunodiagnosis
<b>Abstract:</b>	<p>Background: At present, as a serious zoonotic infectious disease, the incidence of brucellosis is increasing each year worldwide, exhibiting signs of resurgence. Brucellosis seriously threatens the health of humans, and it is necessary to strengthen the methods utilized for its rapid and accurate diagnosis.</p> <p>Methodology/Principal Findings: Bioinformatic technology was used to predict B-cell epitopes of the main outer membrane proteins of Brucella and subsequently verified the antigenicity of these epitopes. Prepared a Brucella multiepitope fusion protein and verified the antigenicity of the protein by indirect ELISA. Whatman filter paper was then modified with nano-zinc oxide to construct a paper-based ELISA (p-ELISA) technology for the diagnosis of brucellosis. A total of 22 linear B cell epitopes were predicted. Each epitope could recognize some brucellosis sera. The constructed multiepitope fusion protein had good antigenicity and significantly reduced cross-reaction compared with LPS. The sensitivity and specificity of the method were 92.38% and 98.35%, the positive predictive value was 98.26%, and the negative predictive value was 91.67%.</p> <p>Conclusions: A multiepitope fusion protein of Brucella was successfully prepared, and a rapid diagnostic technique for brucellosis was established. This technology has potential application value and can be used for the rapid diagnosis of brucellosis.</p>
<b>Additional Information:</b>	
<b>Question</b>	<b>Response</b>
<b>Financial Disclosure</b>  Enter a financial disclosure statement that describes the sources of funding for the work included in this submission. Review the <a href="#">submission guidelines</a> for detailed requirements. View published research articles from <a href="#">PLOS NTDs</a> for specific examples.  This statement is required for submission and <b>will appear in the published article</b> if the submission is accepted. Please make sure it is accurate.	This work was supported by the National Natural Science Foundation of China (Grant number 81802101 , received by Dehui Yin). The funders had no role in study design, data collection and analysis, decision to publish, or preparation of the manuscript.

### Unfunded studies

Enter: *The author(s) received no specific funding for this work.*

### Funded studies

Enter a statement with the following details:

- Initials of the authors who received each award
- Grant numbers awarded to each author
- The full name of each funder
- URL of each funder website
- Did the sponsors or funders play any role in the study design, data collection and analysis, decision to publish, or preparation of the manuscript?
- **NO** - Include this sentence at the end of your statement: *The funders had no role in study design, data collection and analysis, decision to publish, or preparation of the manuscript.*
- **YES** - Specify the role(s) played.

\* typeset

### Competing Interests

Use the instructions below to enter a competing interest statement for this submission. On behalf of all authors, disclose any [competing interests](#) that could be perceived to bias this work—acknowledging all financial support and any other relevant financial or non-financial competing interests.

This statement **will appear in the published article** if the submission is accepted. Please make sure it is accurate. View published research articles from [PLOS NTDs](#) for specific examples.

The authors have declared that no competing interests exist.

**NO authors have competing interests**

Enter: *The authors have declared that no competing interests exist.*

**Authors with competing interests**

Enter competing interest details beginning with this statement:

*I have read the journal's policy and the authors of this manuscript have the following competing interests: [insert competing interests here]*

\* typeset

This statement is **required** for submission and **will appear in the published article** if the submission is accepted. Please make sure it is accurate and that any funding sources listed in your Funding Information later in the submission form are also declared in your Financial Disclosure statement.

**Data Availability**

Authors are required to make all data underlying the findings described fully available, without restriction, and from the time of publication. PLOS allows rare exceptions to address legal and ethical concerns. See the [PLOS Data Policy](#) and [FAQ](#) for detailed information.

Yes - all data are fully available without restriction

A Data Availability Statement describing where the data can be found is required at submission. Your answers to this question constitute the Data Availability Statement and **will be published in the article**, if accepted.

**Important:** Stating 'data available on request from the author' is not sufficient. If your data are only available upon request, select 'No' for the first question and explain your exceptional situation in the text box.

Do the authors confirm that all data underlying the findings described in their manuscript are fully available without restriction?

**Describe where the data may be found in full sentences. If you are copying our sample text, replace any instances of XXX with the appropriate details.**

- If the data are **held or will be held in a public repository**, include URLs, accession numbers or DOIs. If this information will only be available after acceptance, indicate this by ticking the box below. For example: *All XXX files are available from the XXX database (accession number(s) XXX, XXX).*
- If the data are all contained **within the manuscript and/or Supporting Information files**, enter the following: *All relevant data are within the manuscript and its Supporting Information files.*
- If neither of these applies but you are able to provide **details of access elsewhere**, with or without limitations, please do so. For example:

*Data cannot be shared publicly because*

All relevant data are within the manuscript and its Supporting Information files.

of [XXX]. Data are available from the XXX Institutional Data Access / Ethics Committee (contact via XXX) for researchers who meet the criteria for access to confidential data.

The data underlying the results presented in the study are available from (include the name of the third party and contact information or URL).

- This text is appropriate if the data are owned by a third party and authors do not have permission to share the data.

\* typeset

Additional data availability information:



23 E-mail: [jianghai@icdc.cn](mailto:jianghai@icdc.cn).

24 School of Public Health, Xuzhou Medical University, No. 129 Tongshan Road,

25 Xuzhou, 221004, China. E-mail: [xiaopangpeng@126.com](mailto:xiaopangpeng@126.com)

26

27 **Abstract**

28 **Background:** At present, as a serious zoonotic infectious disease, the incidence of  
29 brucellosis is increasing each year worldwide, exhibiting signs of resurgence.  
30 Brucellosis seriously threatens the health of humans, and it is necessary to strengthen  
31 the methods utilized for its rapid and accurate diagnosis.

32 **Methodology/Principal Findings:** Bioinformatic technology was used to predict  
33 B-cell epitopes of the main outer membrane proteins of Brucella and subsequently  
34 verified the antigenicity of these epitopes. Prepared a Brucella multiepitope fusion  
35 protein and verified the antigenicity of the protein by indirect ELISA. Whatman filter  
36 paper was then modified with nano-zinc oxide to construct a paper-based ELISA  
37 (p-ELISA) technology for the diagnosis of brucellosis. A total of 22 linear B cell  
38 epitopes were predicted. Each epitope could recognize some brucellosis sera. The  
39 constructed multiepitope fusion protein had good antigenicity and significantly  
40 reduced cross-reaction compared with LPS. The sensitivity and specificity of the  
41 method were 92.38% and 98.35%, the positive predictive value was 98.26%, and the  
42 negative predictive value was 91.67%.

43 **Conclusions:** A multiepitope fusion protein of Brucella was successfully prepared,  
44 and a rapid diagnostic technique for brucellosis was established. This technology has  
45 potential application value and can be used for the rapid diagnosis of brucellosis.

46 **Keywords:** brucellosis; nano-zinc oxide; p-ELISA; immunodiagnosis

47 **Author Summary**

48 Brucellosis has caused tremendous economic losses in agriculture and husbandry



49 in various countries. Therefore, developing rapid, sensitive and specific diagnostic  
50 techniques for brucellosis has become critical brucellosis research. In this study, a  
51 low-cost diagnostic technique for use in resource-constrained settings was established.  
52 We used immunoinformatic technology to predict the B cell epitopes in the major  
53 outer membrane proteins of Brucella, synthesized polypeptides and coupled them  
54 with KLH, screened these polypeptides by iELISA methods, selected effective  
55 polypeptides as diagnostic antigens, and established a p-ELISA for brucellosis  
56 diagnosis based on a multiepitope fusion protein that can be used to assess the serum  
57 of human.  
58

## 59 **Introduction**

60 Brucellosis is a reemerging zoonotic infectious disease. In recent years, the  
61 incidence rate has been increasing yearly. It not only seriously threatens the health of  
62 the people but also causes huge economic losses to the animal husbandry industry.  
63 Brucellosis has a complex condition and a long course of disease, causing a huge  
64 economic burden and a waste of medical resources in countries all over the world,  
65 especially after misdiagnosis, which will increase the treatment cost[1]. Therefore, the  
66 rapid and accurate diagnosis of brucellosis is necessary. At present, the diagnostic  
67 methods for brucellosis include traditional pathogenic detection, serological  
68 diagnostic techniques and molecular biology methods[2,3].

69 The traditional isolation culture method requires complicated laboratory and  
70 medium conditions, which need to be carried out in a P3 laboratory, and the culture  
71 time is long, usually several weeks[4]. Molecular biology methods such as PCR  
72 technology have specific and rapid characteristics, but nucleic acid contamination will  
73 cause false positive results, the sensitivity and specificity are not high, and it requires  
74 relatively expensive instruments and professional operation, which is not conducive to  
75 popularization in grassroots units[5]. Serological diagnostic techniques mainly  
76 include the agglutination test, complement fixation test (CFT), enzyme-linked  
77 immunosorbent assay (ELISA), immunochromatographic diagnostic test (ICDT), and  
78 fluorescence polarization assay (FPA), which are currently the commonly used  
79 screening methods for brucellosis[6]. This method has the advantages of high  
80 sensitivity and short operation time, but the diagnosis of serological methods is

81 greatly affected by antigens. The key technology to improve the sensitivity and  
82 specificity of serological diagnostic methods is to find suitable diagnostic antigens.  
83 Paper-based enzyme-linked immunosorbent assay (p-ELISA) is an emerging  
84 detection technology. It has the same principle as the traditional 96-well plate ELISA  
85 except that it uses paper as a solid phase carrier. Due to its small reagent dosage, rapid  
86 detection, low cost, and lack of need for special equipment, it has attracted increasing  
87 clinical attention[7,8]. The main advantages of paper as a carrier are as follows: wide  
88 range of paper sources and low cost; through capillary action, no external force is  
89 needed to make the liquid flow; good biocompatibility; small reagent loading volume;  
90 and easy to use and carry[9].

91 In this study, we used immunoinformatic technology to predict the B cell epitopes  
92 in the major outer membrane proteins of Brucella, synthesized polypeptides and  
93 coupled them with KLH, screened these polypeptides by traditional ELISA methods,  
94 selected effective polypeptides as diagnostic antigens, and established a  
95 nano-ZnO-modified p-ELISA for brucellosis diagnosis based on a multiepitope fusion  
96 protein.

## 97 **Methods**

### 98 **Human serum samples**

99 There were 121 human brucellosis sera (gifted by the School of Public Health of  
100 Jilin University), 90 control sera, including 50 healthy sera and 40 patient sera  
101 (confirmed by blood culture to be infected with other pathogens, collected by the  
102 infection department of the First Clinical Hospital of Jilin University; information on

103 the patients is shown in Table S1). All experiments involving human or animal  
104 samples were fully compliant with ethical approval granted by the Animal Care and  
105 Ethics Committee of Xuzhou Medical University.

#### 106 **Selection of the outer membrane proteins of Brucella**

107 The antigenicity of the outer membrane proteins of Brucella was investigated by  
108 consulting the literature (<https://www.ncbi.nlm.nih.gov/protein/>). The amino acid  
109 sequence was obtained, and the conservation of the amino acid sequence was  
110 analyzed by BLAST.

#### 111 **B cell epitope prediction and peptide synthesis**

112 The conserved amino acid sequence of the Brucella outer membrane protein was  
113 used to predict B cell epitopes by using the B cell epitope prediction tool bepiped  
114 linear epitope prediction 2.0 in IEDB (<http://tools.iedb.org/bcell/>). The predicted B  
115 cell epitopes were delivered to SGS and coupled with keyhole limpet hemocyanin  
116 (KLH). The predicted B cell epitope was handed over to Sangon Biotech (Shanghai,  
117 China) for synthesis and coupled with keyhole limpet hemocyanin (KLH).

#### 118 **Screening of peptide epitopes**

119 To screen effective peptide epitopes, we verified the antigenicity of predicted  
120 epitopes by indirect ELISA. The experimental procedure was as follows: peptides  
121 coupled to KLH were diluted with carbonate buffer (pH = 9.6) to final concentrations  
122 of 30 µg/mL and 100 µL/well in a 96-well plate (Corning, USA) and incubated  
123 overnight at 4°C. Next, 300 µL/well of blocking solution (PBS containing 5%  
124 skimmed milk powder) was incubated at 37°C for 1 h, and the cells were washed 3

125 times with PBST (PBS containing 0.05% Tween 20). Afterwards, 100  $\mu$ L/well of  
126 1:400 serum was added and incubated at 37°C for 1 h followed by washing 3 times  
127 with PBST. Next, 1:5000 diluted HRP-labeled protein G (Thermo, USA) was added;  
128 it was reacted at room temperature for 15 min and washed again with PBST 3 times.  
129 Next, 100  $\mu$ L of TMB substrate solution was added to each well and reacted for 15  
130 min at room temperature followed by the addition of 50  $\mu$ L of stop solution (2 M  
131 H<sub>2</sub>SO<sub>4</sub>). The optical density was measured at 450 nm (OD<sub>450</sub>) using an ELISA plate  
132 reader (BioTek, USA). At the same time, KLH (30  $\mu$ g/mL) and lipopolysaccharide  
133 (LPS, 1  $\mu$ g/mL, provided by China Animal Health and Epidemiology Center  
134 (Qingdao, China)) were used as blank carriers and positive antigen controls to detect  
135 serum.

### 136 **Fusion protein preparation**

137 The selected effective peptides are connected in series, and the adjacent two  
138 peptide chains are connected with the linker 'GGGS'. The plasmid was constructed by  
139 full gene synthesis, subcloned into the expression vector pET-21a (Sangon Biotech,  
140 Shanghai, China) and further transformed into E. coli competent BL21(DE3) cells  
141 (Sangon Biotech, Shanghai, China). The cells were cultured, IPTG was used to induce  
142 expression, bacteria were collected, the protein was purified, and the target protein  
143 was verified by SDS-PAGE and Western blotting. The specific steps are described  
144 below.

145 After transferring the recombinant plasmid into BL21(DE3), 800  $\mu$ L of  
146 nonresistant LB medium was added, followed by incubation at 37°C for 45 min and

147 centrifugation at 5000 rpm for 3 min. Most of the supernatant was discarded (leave  
148 approximately 100-150  $\mu\text{L}$ ), the bacteria were resuspended, the LB plate with  
149 corresponding resistance was selected, and it was coated. After air-drying, it was  
150 inverted and cultured overnight in a 37°C incubator. The monoclonal colonies on the  
151 plate were chosen, placed into 10 mL of LB liquid medium and incubated at 37°C and  
152 200 rpm. The cultured bacterial solution was transferred to 750 mL of LB liquid  
153 medium at 37°C and 200 rpm, cultured to  $\text{OD}_{600}=0.6-0.8$  with IPTG (0.5 mM) at  
154 16°C and induced overnight. Then, the cells were centrifuged at 6000 rpm for 5 min,  
155 the supernatant was discarded, and the bacteria were collected. Bacteria were blown  
156 away with 20-30 mL 10 mM Tris-HCl (pH = 8.0) solution and ultrasonically broken  
157 (500 W, 60 times, 10 s each time, 15 s interval). After sonication, 100  $\mu\text{L}$  of the  
158 bacterial suspension was centrifuged at 12000 rpm for 10 min, and 50  $\mu\text{L}$  of  
159 supernatant was transferred to another EP tube. After the supernatant was removed,  
160 the precipitate was blown away with 50  $\mu\text{L}$  of 10 mM Tris-HCl (pH = 8.0) solution.  
161 SDS-PAGE and Western blotting were used to detect protein expression. A nickel  
162 column (Ni Sepharose 6 Fast Flow, GE Healthcare) for affinity chromatography was  
163 used for protein purification. Taking 5 mL of Ni-NTA, the equilibrium column was  
164 washed with 5 times the column bed volume of binding buffer at a flow rate of 5  
165 mL/min. The crude protein was incubated with the equilibrated column packing for 1  
166 h; the incubated product was loaded onto the column and the effluent liquid was  
167 collected; the equilibrium column was washed with binding buffer; the column was  
168 washed with washing buffer, and the effluent liquid was collected; with the column

169 was eluted with elution buffer, and the effluent liquid was collected; and the crude  
170 protein was treated, washed with effluent and eluted with effluent separately, followed  
171 by sample preparation and, SDS-PAGE and WB detection. The concentrated protein  
172 was divided into 1 mL/tube and stored at -80°C.

### 173 **Antigenicity identification of fusion protein**

174 Indirect ELISA was used to verify the antigenicity of the fusion protein. The  
175 procedure was as follows: 96-well microtiter plates were coated with 1 µg/well fusion  
176 protein at 4°C overnight, and then, 5% skimmed milk powder was blocked at 37°C  
177 for 2 h. Serum was diluted 1:400 and added at 100 µL per well, followed by  
178 incubation at 37°C for 1 h. HRP-labeled protein G was diluted with 1:8000, added at  
179 100 µL/well, incubated at 37°C for 1 h, and finally developed with TMB substrate  
180 solution for 15 min. For termination, 2 M H<sub>2</sub>SO<sub>4</sub> was used, and the OD<sub>450</sub> was  
181 measured. After each step, the cells were washed with PBST (0.05% Tween-20 in  
182 PBS) 3 times.

### 183 **Synthesis of nano-ZnO and paper modification**

184 ZnO nanorods were synthesized on Whatman No. 1 filter paper by a  
185 hydrothermal method[10]. The steps were as follows: Whatman filter paper was  
186 soaked in 100 mm zinc acetate solution for 60 s and then annealed at 100 °C for 1 h to  
187 form a seed layer (seed layer). Then, the filter paper with a seed layer was transferred  
188 to a hydrothermal reaction vessel containing an equimolar solution (100 mm, pH =  
189 6.5) of hexamethylenetetramine (HMTA, Sigma) and zinc nitrate (Zn(NO<sub>3</sub>)<sub>2</sub>·6H<sub>2</sub>O,  
190 Sigma). ZnO nanorods were synthesized at 90 °C for 5 h. Next, Whatman filter paper

191 with ZnO nanorods was immersed in anhydrous toluene solution (Sigma) with 1%  
192 APTES (Sigma) for 5 min, heated and dried at 100 °C for 15 min, and silanized.  
193 Scanning electron microscopy (SEM, JSM-7500F), X-ray diffraction (XRD, Bruker  
194 D8) and X-ray photoelectron spectroscopy (XPS, Escalable250Xi) were used to  
195 characterize the structure and surface of the paper. Whatman filter paper modified  
196 with ZnO nanorods was punched into circular paper pieces with a diameter of 10 mm  
197 by a punch, and A4 plastic packaging paper was punched into small holes with a  
198 diameter of 6 mm by a punch. The 10 mm filter paper pieces were placed in the center  
199 of the 6 mm holes of the plastic packaging paper, fixed by a plastic packaging  
200 machine, and cut into small strips with 3 holes for standby.

#### 201 **Establishment of p-ELISA**

202 Five microliters of fusion protein solution was placed in each well (30 µg/mL in  
203 PBS), incubated at room temperature for 30 min, washed with 20 µL of deionized  
204 water 3 times, and blocked with 20 µL of 5% skimmed milk powder at room  
205 temperature for 15 min; PBST was used for washing 3 times, and 5 µL of serum was  
206 added (diluted with 1:400); PBST was used for washing 3 times, and 5 µL of HRP  
207 labeled protein G was added (diluted with 1:8000), followed by incubation at room  
208 temperature for 210 s; and PBST was used for washing 3 times, 5 µL of TMB  
209 substrate solution was developed for 10 min, and an HP Laser Jet Pro MFP M227 was  
210 used for scanning to obtain the image. ImageJ software carries out gray intensity  
211 analysis for quantitative analysis.

#### 212 **Traditional p-ELISA**



213 To compare with the nanomodified p-ELISA (nano-p-ELISA) method, we also  
214 performed the traditional p-ELISA (tra-p-ELISA) method. The specific steps have  
215 been described in the literature[11]. Five microliters of chitosan was added to  
216 deionized water (0.25 mg/mL) and placed onto Whatman No.1 filter paper followed  
217 by drying at room temperature; then 5  $\mu$ L of 2.5% glutaraldehyde solution (PBS) was  
218 added, followed by resting at room temperature for 2 h and washing with 20  $\mu$ L of  
219 deionized water twice. The remaining steps are same as described in section 2.8.

## 220 **Statistical analysis**

221 Dot plot and receiver operating characteristic (ROC) curve analyses were  
222 performed using GraphPad Prism version 6.05 for Windows. The OD450 and gray  
223 intensity were determined by Student's t-test (unpaired t-test). *P*-values < 0.05 were  
224 considered to indicate significant differences.

## 225 **Results**

### 226 **Brucella outer membrane protein epitope prediction and peptide synthesis**

227 Five highly conserved proteins, omp16, omp25, omp31, omp2b and BP26, were  
228 selected. All information on Brucella species and protein accession numbers are  
229 shown in Table S2. A total of 22 epitopes were predicted for the selected proteins, and  
230 the detailed epitope information is shown in Table 1. The 22 polypeptide epitopes  
231 were synthesized and coupled to KLH. KLH was uniformly coupled to the tail end of  
232 the polypeptide (right side). Each polypeptide (10 mg) was coupled to 10 mg of KLH,  
233 and the purity was >90%.

234 Table 1 Detailed information of 22 predicted B cell epitopes

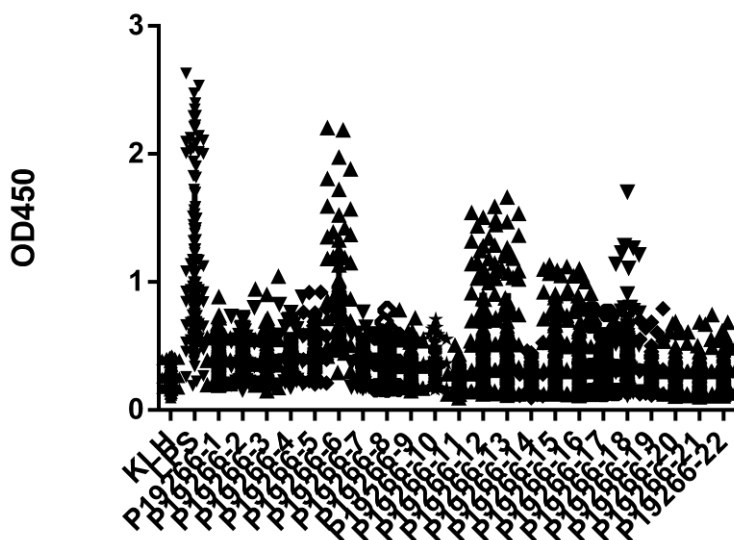
<b>Protein</b>	<b>Epitope (amino acid sequence)</b>	<b>Start-end position</b>	<b>Peptide ID</b>
BP26	AFAQENQMTTQPARIAV	26-42	P19266-1
	KAGIEDRDLQTGGIN	88-100	P19266-2
	QPIYVYPDDKNNLKEPTITGY	104-124	P19266-3
	GVNQGGDLNLVNDNPSAVIN	151-170	P19266-4
	LSRPPMPMP	204-212	P19266-5
	AAAPDNSVPIAAGENSYNVSVNVVFE	223-248	P19266-6
Omp2b	SGAQAADAIVAPEPEAVEY	31-49	P19266-7
	DVKGGDDVYSGTDRNGWDK	79-97	P19266-8
	NNSGVDGKYGNETSSGTV	129-146	P19266-9
	TVTPEVSYTKFGGEWKNTVAEDNAWGGI	341-368	P19266-10
Omp16	AAAPGSSQDFTV	44-55	P19266-11
	SRGVPTNRMRTISYGNERPVAVCD	125-148	P19266-12
Omp25	GRAKLENRTNGGTS	56-69	P19266-13
	GNPVQTTGETQ	115-125	P19266-14
	GGIKNSLRIGGEESKSKTQT	154-174	P19266-15
	GWTVGAGIEYAA	175-186	P19266-16
	TDYGKKNFGLNDLDTRGSFKTNDIR	199-223	P19266-17
Omp31	VSEPSAPTAAPVDTF SWTGGYIGINA	24-49	P19266-18
	GKFKHPFSSFDKEDNEQVSGSL	53-75	P19266-19
	TGSISAGASGLEGKAE	112-127	P19266-20

GDDASALHTWSDKTKAGWTLGAGAEYA	168-194	P19266-21
DLGKRNLVD	109-217	P19266-22

235

236 **Peptide screening**

237 The KLH-conjugated polypeptide was used as the antigen, and the indirect  
 238 ELISA method was used to verify the antigenicity of the polypeptide. Positive serum  
 239 was used to screen the polypeptide. The results of iELISA show that each peptide can  
 240 recognize some sera, and the recognition ability is quite different (see Fig 1).



241

242 **Fig 1.** The results of iELISA of each peptide identification-positive brucellosis serum

243

244 **Fusion protein preparation**

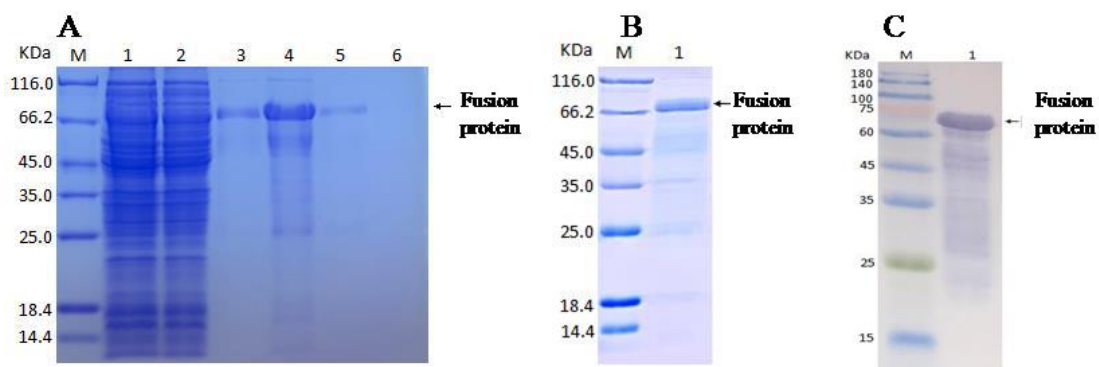
245 SDS-PAGE identification results showed that after 0.5 mM IPTG-induced  
 246 expression overnight, the expression of the fusion protein reached an ideal amount,  
 247 and the expression molecular weight was approximately 66 kDa. The results are  
 248 shown in Fig. 2A and Fig. 2B. After Western blot identification and analysis, the

249 molecular weight of the histidine tag was consistent with the SDS-PAGE results, and  
250 after mass spectrometry verification, it was confirmed that the expressed protein was  
251 the target protein. The detailed results are shown in Fig. 2C.

252

### 253 **Antigenicity identification of fusion protein**

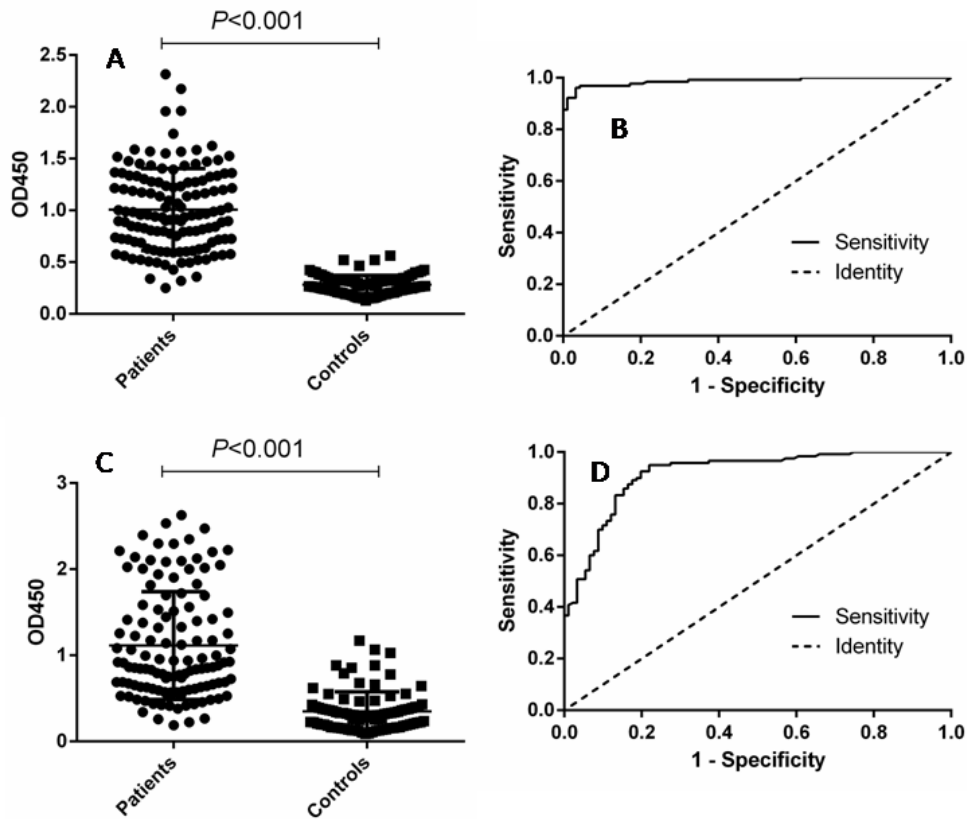
254 The antigenicity of the purified fusion protein was verified by iELISA. Compared  
255 with the LPS antigen, the area under the diagnostic curve of the fusion protein was  
256 0.9877 (95% CI: 0.9758 to 0.9996), while the area under the LPS curve was 0.9174  
257 (95% CI: 0.8796 to 0.9552) (the results are shown in Fig. 3). The optimal cutoff value  
258 was calculated by the Youden index, the positive predictive value and negative  
259 predictive value of the fusion protein were higher than those of LPS, and the  
260 diagnostic predictive value of the two antigens under this cutoff value was analyzed  
261 (Table 2).



262

263 **Fig. 2** SDS-PAGE and Western blot analysis of fusion proteins. (A) SDS-PAGE  
264 identification results after IPTG-induced expression overnight (M, marker; lane1,  
265 loading solution; lane2, flow-through solution; lane3-4, 20 mM imidazole elution  
266 fraction; lane5, 50 mM imidazole elution fraction; lane6, 500 mM imidazole elution

267 fraction). (B) SDS-PAGE identification results of purified fusion protein (M, marker;  
 268 lane1, purified protein). (C) Western blot results of purified protein (M, marker; lane1,  
 269 purified protein).



270  
 271 **Fig. 3** ELISA analysis of human serum samples. (A) Dotplot of the fusion protein  
 272 ELISA assay. (B) ROC analysis of fusion protein IELISA assay results. (C) Dotplot of  
 273 the LPS antigen ELISA assay. (D) ROC analysis of LPS antigen ELISA assay results.  
 274  
 275 Table 2. Positive and negative predictive values of the test calculated for different  
 276 cutoff values

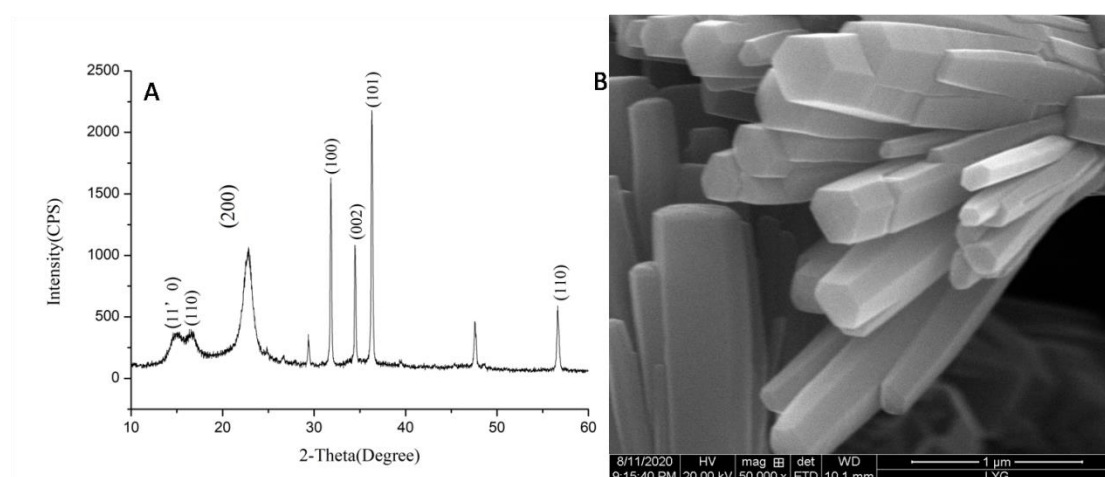
Cutoff value	Positive		Negative		PPV (%)	NPV (%)
	TP	FN	TN	FP		

$\geq 0.470$ (fusion protein)	117	4	87	3	95.90	95.51
$\geq 0.4095$ (LPS)	115	6	70	20	85.19	92.10
$\geq 50.98$ (nano-p-ELISA)	113	8	88	2	98.26	91.67
$\geq 45.66$ (tra-p-ELISA)	113	8	87	3	97.41	91.58

277 TP, true positives; TN, true negatives; FP, false positives; FN, false negatives; PPV,  
 278 positive predictive value  $(TP/TP+FP) \times 100$ ; NPV, negative predictive value  
 279  $(TN/TN+FN) \times 100$ .

## 280 Synthesis and characterization of nano-ZnO

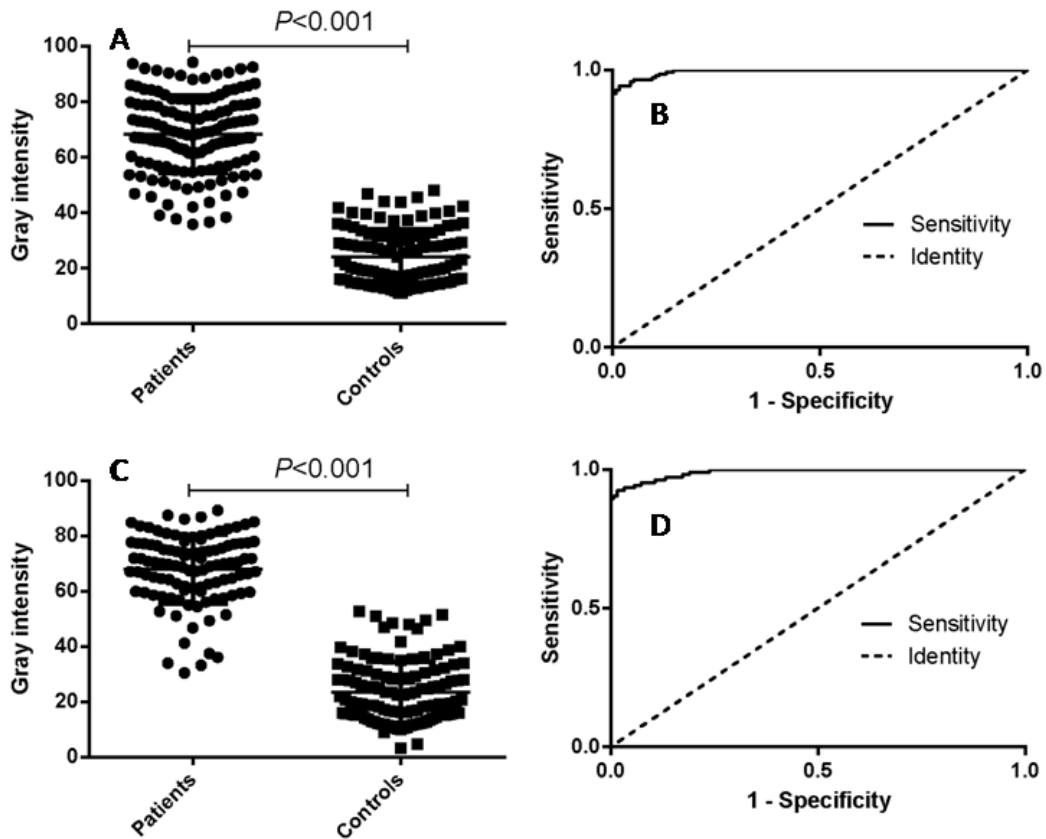
281 Scanning electron microscopy showed that we synthesized nano-zinc oxide on  
 282 the surface of Whatman filter paper (Fig. 4B). At the same time, XRD results showed  
 283 that the functionalization of nano-zinc oxide was successfully performed (Fig. 4A).  
 284 XPS shows that the concentration of Zn atoms is 40.79% and the concentration of  
 285 oxygen atoms is 59.21%, which further indicates that the concentration of zinc and  
 286 oxygen in the sample is ZnO.



287  
 288 **Fig. 4** Nano-ZnO characterization results. (A) XRD results. (B) Scanning electron  
 289 microscope results.

290 **Evaluation of the diagnostic effect of p-ELISA**

291 A total of 211 sera were detected by the p-ELISA method modified by nano-ZnO  
292 (nano-p-ELISA) and the p-ELISA method modified by chitosan and glutaraldehyde  
293 (tra-p-ELISA) to evaluate the diagnostic effects of the two methods. The gray  
294 intensity of 121 brucellosis-positive sera and 90 brucellosis-negative sera was  
295 analyzed by ROC curve analysis, and the results of the nano-p-ELISA showed that the  
296 area under the curve was 0.9900 (95% CI, 0.9816 to 0.9984), indicating that the  
297 diagnosis of this method has a very high accuracy. The optimal cutoff value was  
298 50.98. Under this cutoff value, the sensitivity of this method was 92.38% (95% CI,  
299 0.8554 to 0.9665) and the specificity was 98.35% (95% CI, 0.9416 to 0.9980) (Fig.  
300 5A). Using this optimal cutoff value to further analyze the diagnostic effect, 113 of  
301 the 121 positive samples were accurately diagnosed, and 88 of the 90 negative  
302 samples were correct. The positive predictive value of the nano-p-ELISA was 98.26%,  
303 and the negative predictive value was 91.67% (Table 2). The gray intensities of the  
304 positive and negative samples were significantly different ( $P<0.001$ ) (Fig. 5B).



305

306 **Fig. 5** P-ELISA analysis of human serum samples. (A) Dotplot of the nano-p-ELISA  
 307 assay. (B) ROC analysis of nano-p-ELISA assay results. (C) Dotplot of the  
 308 tra-p-ELISA assay. (D) ROC analysis of tra-p-ELISA assay results.

309 The results of the tra-p-ELISA showed that the area under the curve was 0.98.94  
 310 (95% CI, 0.9817 to 0.9970), indicating that the diagnosis of this method also has high  
 311 accuracy. The optimal cutoff value is 45.66. Under this cutoff value, the diagnostic  
 312 sensitivity of this method was 94.24% (95% CI, 0.8897 to 0.9748), and the specificity  
 313 was 98.26% (95% CI, 0.9386 to 0.9979) (Fig. 5C). With this optimal cutoff value,  
 314 113 of the 121 positive samples were accurately diagnosed, and 87 of the 90 negative  
 315 samples were correctly judged as negative. The positive predictive value of the  
 316 tra-p-ELISA was 97.41%, and the negative predictive value was 91.58% (Table 2).



317 The gray intensities of the positive and negative samples were significantly different  
318 ( $P < 0.001$ ) (Fig. 5D).

### 319 **Discussion**

320 The existing diagnostic methods for brucellosis have disadvantages such as  
321 complicated operation, long time consumption, low sensitivity, and proneness to  
322 cross-reaction[12]. Therefore, a simple, fast and sensitive diagnostic method is sought.  
323 Early diagnosis and early treatment of the disease are of great significance to reduce  
324 economic loss and medical burden[13]. The development of new diagnostic  
325 techniques for brucellosis is of great significance for the prevention and control of  
326 brucellosis.

327 At present, many vaccine studies have shown that many outer membrane proteins  
328 in *Brucella* have strong antigenicity[14-16]. Animal experiments have also shown that  
329 these ingredients have a certain immunoprotective effect on *Brucella* and are good  
330 vaccine candidates[17,18]. Therefore, these components also provide a direction for  
331 researchers to develop new diagnostic antigens for brucellosis, and the development  
332 of immunoinformatic technology provides tools for the development of new  
333 diagnostic antigens. Immunoinformatic is based on bioinformatic tools, an emerging  
334 science that integrates life sciences, computer science, and mathematics[19,20].  
335 Immunoinformatic technology uses bioinformatic tools to treat pathogens without  
336 cultivating them. Processing and analysis of, for instance, the genome and proteome  
337 can be used to complete the gene prediction and the prediction of cell epitopes in the  
338 protein[21]. Immunoinformatic technology has the advantages of speed and economy

339 and has been widely used in vaccine design, disease prevention, diagnosis and  
340 treatment. In this study, we selected five Brucella antigen proteins, omp16, omp25,  
341 omp31, omp2b and BP26, and predicted 22 epitopes. The results of iELISA  
342 confirmed that each peptide can recognize a portion of brucellosis sera, but the  
343 recognition ability of each polypeptide is limited. Therefore, we concatenated 22  
344 epitopes to synthesize a fusion protein. Using the fusion protein as an antigen, the  
345 ability to recognize serum is greatly improved. Compared with LPS, the use of fusion  
346 proteins can significantly reduce serological cross-reactions.

347 P-ELISA has attracted the attention of many researchers due to its advantages,  
348 such as strong specificity, simplicity, rapidity, portability, and low cost, especially in  
349 the fields of medical testing, environmental testing and food safety analysis[22,23]. It  
350 combines the advantages of traditional ELISA and paper and provides a new method  
351 and new idea for resource-poor areas and point-of-care testing. At present, the  
352 commonly used p-ELISA is a method of modifying the surface of paper with  
353 glutaraldehyde and chitosan. Currently, nanomaterials have the characteristics of a  
354 large specific surface area and quantum size effect and have been widely used in the  
355 fields of biology and medicine[24,25]. The modification of nanomaterials on the  
356 surface of paper can increase the surface area of the paper and establish a p-ELISA  
357 diagnostic method for nanomaterial modification[10,26]. In this study, we modified  
358 the surface of paper with nano-ZnO and used a synthetic fusion protein as the antigen  
359 to establish a new diagnostic technique for brucellosis. The diagnostic effect is good,  
360 and it can be modified with glutaraldehyde and chitosan. The p-ELISA diagnostic

361 method is comparable. In addition, p-ELISA paper modified by nanomaterials can be  
362 stored at room temperature for a long time, and we also found in experiments that the  
363 color development time of p-ELISA modified by nanomaterials can be significantly  
364 extended, which may be due to the antioxidant effect of nanomaterials, thus extending  
365 the effective time of the color reagent. Compared with the traditional ELISA method,  
366 the p-ELISA diagnostic method uses very few reagents and shortens the time for the  
367 entire process. It is a relatively promising on-site rapid detection technology.

368 In summary, using bioinformatic technology combined with nanomaterials, this  
369 performance has established a new type of brucellosis diagnostic technology, which  
370 has good potential application value. However, the brucellosis sera selected in this  
371 study were all clinically screened positive sera, and the number was limited. The  
372 diagnostic validity of this method requires a large number of clinical random samples  
373 for verification.

374

#### 375 **Acknowledgments**

376 Not applicable

#### 377 **Competing interests**

378 The authors declare that they have no competing interests

#### 379 **Funding**

380 This work was supported by the National Natural Science Foundation of China (Grant  
381 number 81802101). The funders had no role in study design, data collection and  
382 analysis, decision to publish, or preparation of the manuscript.

383

#### 384 **References**

- 385 1. Olsen SC, Palmer MV. Advancement of knowledge of *Brucella* over the past 50  
386 years. *Vet Pathol.* **2014**; 51:1076-89.
- 387 2. Pappas G, Papadimitriou P, Akritidis N, Christou L, Tsianos EV. The new global  
388 map of human brucellosis. *Lancet Infect Dis.* **2006**;6:91-9.
- 389 3. Dean AS, Crump L, Greter H, Schelling E, Zinsstag J. Global burden of human  
390 brucellosis: a systematic review of disease frequency. *PLoS Negl Trop Dis.*  
391 **2012**;6:e1865.
- 392 4. Araj GF. Update on laboratory diagnosis of human brucellosis. *Int J Antimicrob*  
393 *Agents.* **2010**;36 Suppl 1:12-7.
- 394 5. Zeybek H, Acikgoz ZC, Dal T, Durmaz R. Optimization and validation of a  
395 real-time polymerase chain reaction protocol for the diagnosis of human brucellosis.  
396 *Folia Microbiol (Praha).* **2020**;65:353-61.
- 397 6. Yagupsky P, Morata P, Colmenero JD. Laboratory Diagnosis of Human Brucellosis.  
398 *Clin Microbiol Rev.* **2019**;33:e00073-19.
- 399 7. Zhao Y, Zeng D, Yan C, Chen W, Ren J, Jiang Y, et al. Rapid and accurate detection  
400 of *Escherichia coli* O157:H7 in beef using microfluidic wax-printed paper-based  
401 ELISA. *Analyst.* **2020**;145:3106-15.

- 402 8. Kasetsirikul S, Umer M, Soda N, Sreejith KR, Shiddiky MJA, Nguyen NT.  
403 Detection of the SARS-CoV-2 humanized antibody with paper-based ELISA. *Analyst*.  
404 **2020**;145:7680-86.
- 405 9. Cheng CM, Martinez AW, Gong J, Mace CR, Phillips ST, Carrilho E, et al.  
406 Paper-based ELISA. *Angew Chem Int Ed Engl*. **2010**;49:4771-4.
- 407 10. Tiwari S, Vinchurkar M, Rao VR, Garnier G. Zinc oxide nanorods functionalized  
408 paper for protein preconcentration in biodiagnostics. *Sci Rep*. **2017**;7:43905.
- 409 11. Wang S, Ge L, Song X, Yu J, Ge S, Huang J, et al. Paper-based  
410 chemiluminescence ELISA: lab-on-paper based on chitosan modified paper device  
411 and wax-screen-printing. *Biosens Bioelectron*. **2012**;31:212-8.
- 412 12. Nielsen K, Yu WL. Serological diagnosis of brucellosis. *Prilozi*. **2010**;31:65-89.
- 413 13. Vered O, Simon-Tuval T, Yagupsky P, Malul M, Cicurel A, Davidovitch N. The  
414 Price of a Neglected Zoonosis: Case-Control Study to Estimate Healthcare Utilization  
415 Costs of Human Brucellosis. *PLoS One*. **2015**;10:e0145086.
- 416 14. Hou H, Liu X, Peng Q. The advances in brucellosis vaccines. *Vaccine*. **2019**;  
417 37:3981-8.
- 418 15. Verdiguél-Fernández L, Oropeza-Navarro R, Ortiz A, Robles-Pesina MG,  
419 Ramírez-Lezama J, Castañeda-Ramírez A, et al. *Brucella melitensis* omp31 Mutant Is  
420 Attenuated and Confers Protection Against Virulent *Brucella melitensis* Challenge in  
421 BALB/c Mice. *J Microbiol Biotechnol*. **2020**;30:497-504.
- 422 16. Gupta S, Singh D, Gupta M, Bhatnagar R. A combined subunit vaccine  
423 comprising BP26, Omp25 and L7/L12 against brucellosis. *Pathog Dis*. **2019**;

424 77:ftaa002.

425 17. Rezaei M, Rabbani-Khorasgani M, Zarkesh-Esfahani SH, Emamzadeh R, Abtahi

426 H. Prediction of the Omp16 Epitopes for the Development of an Epitope-based

427 Vaccine Against Brucellosis. *Infect Disord Drug Targets*. **2019**;19:36-45.

428 18. Degos C, Hysenaj L, Gonzalez-Espinoza G, Arce-Gorvel V, Gagnaire A,

429 Papadopoulos A, et al. Omp25-dependent engagement of SLAMF1 by *Brucella*

430 *abortus* in dendritic cells limits acute inflammation and favours bacterial persistence

431 *in vivo*. *Cell Microbiol*. **2020**;22:e13164.

432 19. D'Annessa I, Di Leva FS, La Teana A, Novellino E, Limongelli V, Di Marino D.

433 Bioinformatics and Biosimulations as Toolbox for Peptides and Peptidomimetics

434 Design: Where Are We? *Front Mol Biosci*. **2020**;7:66.

435 20. Agyei D, Tsopmo A, Udenigwe CC. Bioinformatics and peptidomics approaches

436 to the discovery and analysis of food-derived bioactive peptides. *Anal Bioanal Chem*.

437 **2018**;410:3463-72.

438 21. Backert L, Kohlbacher O. Immunoinformatics and epitope prediction in the age of

439 genomic medicine. *Genome Med*. **2015**;7:119.

440 22. Fu H, Song P, Wu Q, Zhao C, Pan P, Li X, et al. A paper-based microfluidic

441 platform with shape-memory-polymer-actuated fluid valves for automated multi-step

442 immunoassays. *Microsyst Nanoeng*. **2019**;5:50.

443 23. Pang B, Zhao C, Li L, Song X, Xu K, Wang J, et al. Development of a low-cost

444 paper-based ELISA method for rapid *Escherichia coli* O157:H7 detection. *Anal*

445 *Biochem*. **2018**; 542:58-62.

446 24. Cui H, Song W, Cao Z, Lu J. Simultaneous and sensitive detection of dual DNA  
447 targets via quantum dot-assembled amplification labels. *Luminescence*. **2016**;  
448 31:281-7.

449 25. Tian Y, Zhang L, Wang L. DNA-Functionalized Plasmonic Nanomaterials for  
450 Optical Biosensing. *Biotechnol J*. **2020**;15:e1800741.

451 26. Marie M, Manoharan A, Kuchuk A, Ang S, Manasreh MO. Vertically grown zinc  
452 oxide nanorods functionalized with ferric oxide for in vivo and non-enzymatic  
453 glucose detection. *Nanotechnology*. **2018**;29:115501.

454

455 **Supporting information**

456

**Table S1** Information of the patient

Order No.	Blood culture serial number	Pathogens
1	200707B0000035	<i>Pseudomonas putida</i>
2	200706B0000086	<i>Aeromonas sobria</i>
3	200705B0000069	<i>Staphylococcus haemolyticus</i>
4	200706B0000032	<i>Escherichia coli</i>
5	200704B0000100	<i>Staphylococcus aureus</i>
6	200708B0000072	<i>Klebsiella pneumoniae</i>
7	200708B0000168	<i>Escherichia coli</i>
8	200708B0000113	<i>Staphylococcus saprophyticus</i>
9	200708B0000051	<i>Moraxella osloensis</i>
10	200709B0000026	<i>Staphylococcus hominis</i>
11	200709B0000099	<i>Raoultella ornithinolytica</i>
12	200714B0000016	<i>Escherichia coli</i>
13	200713B0000052	<i>Escherichia coli</i>
14	200711b0000011	<i>Candida parapsilosis</i>
15	200715B0000042	<i>Staphylococcus aureus</i>
16	200715B0000014	<i>Escherichia coli</i>
17	200714B0000045	<i>Staphylococcus epidermidis</i>
18	200720B0000036	<i>Klebsiella pneumoniae</i>



---

19	200721B0000130	Streptococcus
20	200722B0000005	Pseudomonas aeruginosa
21	200722B0000074	Streptococcus constellatus
22	200726B0000056	Pseudomonas aeruginosa
23	200726B0000039	Rothia mucilaginos
24	200726B0000105	Enterococcus faecium
25	200726B0000040	Staphylococcus hominis
26	200725B0000017	Klebsiella pneumoniae
27	200727B0000068	Escherichia coli
28	200727B0000065	Staphylococcus aureus
29	200724B0000116	Escherichia coli
30	200728B0000078	Enterococcus faecium
31	200728B0000030	Escherichia coli
32	200727B0000128	Escherichia coli
33	200801B0000030	Enterococcus faecium
34	200802B0000001	Staphylococcus aureus
35	200801B0000108	Staphylococcus aureus
36	200803B0000007	Pseudomonas aeruginosa
37	200805B0000057	Staphylococcus aureus
38	200804B0000088	Streptococcus dysgalactiae
39	200804B0000051	Escherichia coli
40	200805B0000125	Escherichia coli

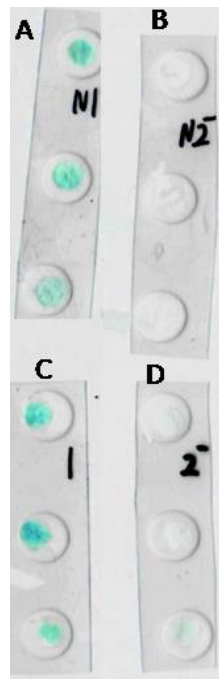
---

457

458 **Table S2.** The OMPs' Accession Numbers of Brucella. in NCBI Protein database

OMPs	Accession Numbers of <i>Brucella</i> spp.		
	<i>B. melitensis</i>	<i>B. abortus</i>	<i>B. suis</i>
BP26	AAB38523.1	AAO39773.1	KFJ31678.1
Omp16	AEF59023.1	AGI97133.1	AIB29945.1
Omp25	AEF59022.1	AFJ79953.1	AHN46339.1
Omp31	ACS50328.1	-	AAL27290.1
Omp2b	AMM72579.1	SUW28200.1	SUW48930.1

459



460

461 Figure S1 Results of p-ELISA. (A) Positive of nano-p-ELISA. (B) Negative of

462 nano-p-ELISA. (C) Positive of tra-p-ELISA. (D) Negative of tra-p-ELISA.

463